



## Leveraging probe data to assess left-turn driver behaviour under varying permissive signals

Xi Zhang, Henrick Haule & Yao-Jan Wu

To cite this article: Xi Zhang, Henrick Haule & Yao-Jan Wu (18 Jun 2025): Leveraging probe data to assess left-turn driver behaviour under varying permissive signals, Transportmetrica A: Transport Science, DOI: [10.1080/23249935.2025.2514664](https://doi.org/10.1080/23249935.2025.2514664)

To link to this article: <https://doi.org/10.1080/23249935.2025.2514664>



Published online: 18 Jun 2025.



Submit your article to this journal [↗](#)



Article views: 38



View related articles [↗](#)



View Crossmark data [↗](#)



# Leveraging probe data to assess left-turn driver behaviour under varying permissive signals

Xi Zhang<sup>a</sup>, Henrick Haule<sup>b</sup> and Yao-Jan Wu<sup>a</sup>

<sup>a</sup>Department of Civil and Architectural Engineering and Mechanics, University of Arizona, Tucson, AZ, USA;

<sup>b</sup>Department of Civil and Environmental Engineering, University of Alabama in Huntsville, Huntsville, AL, USA

## ABSTRACT

Flashing yellow arrows (FYAs) and circular green signals (CGs) are prevalent permissive left-turn indications at intersections. These signals can significantly influence drivers' left-turn behaviour and, in turn, affect intersection safety. Despite this, few studies have investigated differences in left-turn behaviour under these indications. This study leverages probe data to assess speeds, accelerations, and decelerations at 106 FYA and 116 CG intersection approaches in Tucson, Arizona, while controlling for geometric and temporal factors. Results showed that FYA approaches generally exhibited lower speeds and higher decelerations than CGs. Vehicles in the outer lanes of dual left-turn approaches with FYAs showed greater acceleration fluctuations. Additionally, vehicles on dual left-turn lanes, particularly with FYAs, exhibited lower average speeds than those on single left-turn approaches. These findings enhance the understanding of how FYAs and CGs affect driver behaviour at approaches with varying geometric configurations, aiding transportation agencies in making informed decisions to improve intersection safety.

## ARTICLE HISTORY

Received 26 September 2024



Accepted 28 May 2025

## KEYWORDS

Left-turn safety; driver behaviour; flashing yellow arrow; probe data; permissive left-turn indication

## 1. Introduction

Signalised intersections accounted for approximately 34% (4047) of intersection-related fatalities in the United States in 2021 (FHWA 2024). Many of these fatalities are associated with left-turning vehicles, due to their conflicts with oncoming and pedestrians at intersections (Ma and Zhu 2021). Such conflicts can lead to severe crashes, including angle crashes, head-on collisions, and vehicle-to-pedestrian collisions (Abou-Senna et al. 2023). A protected-only left-turn phasing is designed to improve intersection safety by preventing left-turn traffic conflicts. Due to the inefficiency of the protected-only mode in balancing safety and mobility, the protected-permissive left-turn (PPLT) mode has been widely adopted (Appiah et al. 2020; Schattler et al. 2015; Zhang, Li, and Wu 2023). In a PPLT mode, left-turning vehicles have the right-of-way during the protected phase, indicated by a green arrow. During the permissive phase of the PPLT mode, left turns are allowed but must yield

**CONTACT** Xi Zhang  xizhang1@arizona.edu  Department of Civil and Architectural Engineering and Mechanics, University of Arizona, 1209 East 2nd Street, Tucson, AZ 85721, USA

to oncoming traffic and pedestrians, signalled by a flashing yellow arrow (FYA) or a circular green signal (CG). Previous studies have demonstrated that FYAs provide a flexible left-turn control mode that can be dynamically adjusted in response to real-time traffic conditions (Abou-Senna et al. 2014, 2021, 2023).

Drivers' comprehension of the permissive left-turn indications (CGs and FYAs) is critical because a lack of this understanding can result in a failure to yield to oncoming traffic and pedestrians (Zhao et al., 2023). Previous research has shown that drivers better understand FYAs than CGs, leading to relatively fewer crashes at intersections with FYAs (Appiah et al., 2018; Schattler et al. 2015; Srinivasan et al., 2018; Zhang, Li, and Wu 2023). Analysing differences in driver behaviour during permissive left turns with FYAs and CGs can offer insights into the safety impacts of these signals and the mechanisms behind crashes, avoidance, and severity. Most empirical studies on driver behaviour measure parameters, such as traffic gap sizes and vehicle accelerations or decelerations, using survey or video footage (X. Li et al. 2023, 2024; Rescot et al. 2015; Rietgraf and Schattler 2013; Schattler et al. 2013). While these studies have provided insights into driver behaviour in response to different signal phasings, relying on manual data collection, such as video extraction and field observations, limits scalability, as evidenced by the small sample sizes and restricted study sites (Hurwitz et al. 2014; Knodler et al. 2005; Schattler et al. 2013).

The increased availability of high-resolution probe data provides an opportunity to analyse the network-wide impact of FYAs and CGs on left-turn driver behaviour through empirical data (Kandiboina et al. 2024). Most new vehicles have inertial sensors that can report geolocations, speeds, accelerations, and others in near real-time to cloud infrastructure (Islam et al. 2023). This offers a cost-effective and flexible way to collect probe data on a large scale (P. Li et al. 2020). The probe data has been used for various applications, including traffic conflict evaluation and prediction on freeways and at signalised intersections (Islam et al. 2023; Islam and Abdel-Aty 2023; P. Li et al. 2020), roadway hazard identification (H. Li et al. 2020), and work zone safety evaluation (Mathew et al. 2022). Although previous research has utilised probe data to assess hard acceleration rates at intersections where a PPLT mode was converted to a protected-only mode (Saldivar-Carranza et al. 2021), probe data have not yet been used to evaluate driver behaviour in response to different permissive left-turn indications (FYAs and CGs).

This study aims to address the gaps mentioned above with two objectives. First, it demonstrates the use of emerging probe data to capture left-turn behaviour at the lane level. The data processing framework developed in this study can serve as a foundation for researchers to conduct similar evaluations across various traffic scenarios, such as right-turn behaviour at signalised intersections, lane-changing behaviour, and other nuanced traffic movements.

Second, this study conducts individual-level safety assessments comparing driver behaviour with FYAs and CGs through empirical data. This study emphasises the differences in driver behaviour at both single and dual left-turn lanes with FYAs and CGs. Such an examination can provide insights into left-turn phasing at dual left-turn approaches, even though the current recommendation is to use a protected-only left-turn mode at these approaches for safety reasons (Rodegerdts et al. 2004; Zhang, Li, and Wu 2023). The findings can assist practitioners in making informed decisions about existing and future deployments of FYAs.

## 2. Literature review

### 2.1. Left-turn behaviour at signalised intersections

Previous research on left-turn behaviour at signalised intersections focused on driver aggressiveness and gap acceptance (Alhajyaseen, Asano, and Nakamura 2013; Chan 2006; Wang et al. 2023; Yan and Radwan 2007). Wang et al. (2023) categorised left-turn behaviour into no-interference, yield, and rush patterns and identified the rush pattern as the most hazardous (Wang et al. 2023). Alhajyaseen, Asano, and Nakamura (2013) found that drivers accepted shorter gaps when near-side pedestrians were present compared to far-side pedestrians (Alhajyaseen, Asano, and Nakamura 2013). Yan and Radwan (2007) examined the impact of restricted sight distances on driver behaviour, revealing that sight obstructions from opposing vehicles increased critical gaps and follow-up times (Yan and Radwan 2007). The field observations conducted by Chan (2006) indicated that the length of signal phases, vehicle speed and volume, and pedestrian presence influenced gap acceptance (Chan 2006).

Few studies have investigated left-turn behaviour at intersections with FYAs (Rescot et al. 2015; Rietgraf and Schattler 2013; Schattler et al. 2013). Rescot et al. (2015) collected vehicle speeds at two intersections using radar guns, analysed accelerations and decelerations as vehicles approached FYAs, and compared the data with that from two control intersections where doghouse-style signals were used. The results showed no statistically significant differences in accelerations and decelerations between the intersections with FYAs and those with CGs (Rescot et al. 2015). This study was limited by the small number of study sites due to labour-intensive data collection and the lack of rigorous statistical analysis.

Schattler et al. (2013) reviewed 128 h of video footage collected at 16 study sites in Illinois to evaluate the effects of converting from CGs to FYAs. This study concluded that no significant differences were observed in the size of accepted median gaps (Schattler et al. 2013). Rietgraf and Schattler (2013) reviewed four hours of data recorded at six intersections, examining accepted and rejected gap sizes and driver actions (e.g. whether the driver proceeded through the left turn without slowing or stopping) from video recordings. Z-tests and F-tests were used to assess the significance of differences between these variables at intersections with FYAs and those with CGs. The findings indicated that FYAs were associated with the highest combined response rate for safe and efficient actions, including slow or stop, and the acceptance or rejection of adequate gaps (Rietgraf and Schattler 2013). While these studies provide valuable insights into driver behaviour at intersections, they are limited by the availability of video footage and the number of study sites. Additionally, many overlook factors that can influence behaviour at intersections, such as the number of left-turn lanes, opposing through lanes, speed limits, and opposing through speeds.

### 2.2. Probe data for driver behaviour evaluation

Limited studies have employed probe data for safety assessments related to driver behaviour. Saldivar-Carranza et al. (2021) analysed over 7000 vehicle trajectories collected on weekdays in Indiana to investigate the impact of converting a PPLT to a protected-only left-turn mode on hard accelerations. The results showed that most hard accelerations

occurred 16 ft before and up to 50 ft after the stop bar, with a 14% decrease in hard accelerations beyond the stop bar after the left-turn mode changed (Saldivar-Carranza et al. 2021).

Some research has used probe data to evaluate how driver behaviour relates to both traffic conflicts and crash frequency (Hunter et al. 2012; Islam and Abdel-Aty 2023; P. Li et al. 2020). P. Li (2020) and Islam et al. (2023) employed a long short-term memory (LSTM) neural network to predict real-time crash potential and traffic conflict using connected vehicle emulated data and probe data, respectively (Islam and Abdel-Aty 2023; P. Li et al. 2020). Islam et al. found that accelerations above  $0.3 \text{ m/s}^2$ , decelerations between  $-1.5$  and  $-0.25 \text{ m/s}^2$ , and speeds over 30 mph induced traffic conflicts (Islam and Abdel-Aty 2023). They also estimated the time to collision from probe data, evaluating the impact of vehicle dynamics, and geometric and non-geometric roadway attributes on time to collision. The results indicated traffic conflict probability increased by 8% when absolute accelerations exceeded  $0.8 \text{ m/s}^2$  (Islam et al. 2023). Moreover, Hunter et al. found a strong correlation between hard-braking events and rear-end crashes occurring more than 400 ft upstream of an intersection (Hunter et al. 2012).

None of the previous studies have employed probe data to evaluate the impact of FYAs on left-turn driver behaviour, explicitly concerning average speeds, accelerations, and decelerations when entering and leaving intersections. Additionally, no study has evaluated the impact of FYAs on inner and outer lanes at dual left turn lanes. Such analysis can help practitioners better understand the safety implications of FYAs on approaches with dual left-turn lanes. This study thoroughly demonstrated the feasibility of using probe data to evaluate left-turn behaviour in response to FYAs and CGs.

### 3. Data description and processing

#### 3.1. Study locations

This study was based on 61 intersections in Tucson, Arizona, as shown in Figure 1. Considering the signal indication is provided per approach, this study included 106 and 116 approaches with the PPLT-FYA mode and PPLT-CG mode, respectively. The FYA is displayed in a four-section signal head with a supplemental traffic sign with the text 'Left Turn Yield on Flashing Yellow Arrow,' and the CG is displayed in a five-section signal head. All approaches were running a lagging left-turn phasing in 2021.

#### 3.2. Data description

Four datasets, including probe data, traffic controller event-based data, speed data, and geometric characteristics, were used in the analysis. All datasets were collected from January to March 2021, during which time the probe data provided by the Pima Association of Governments (PAG) was available.

##### 3.2.1. Probe vehicle data

The probe data used in this study was collected by Wejo and provided by PAG. This dataset comprises noncommercial fleet data with information, including anonymous unique trajectory identifiers, Global Positioning System (GPS) locations, vehicle travel directions, and

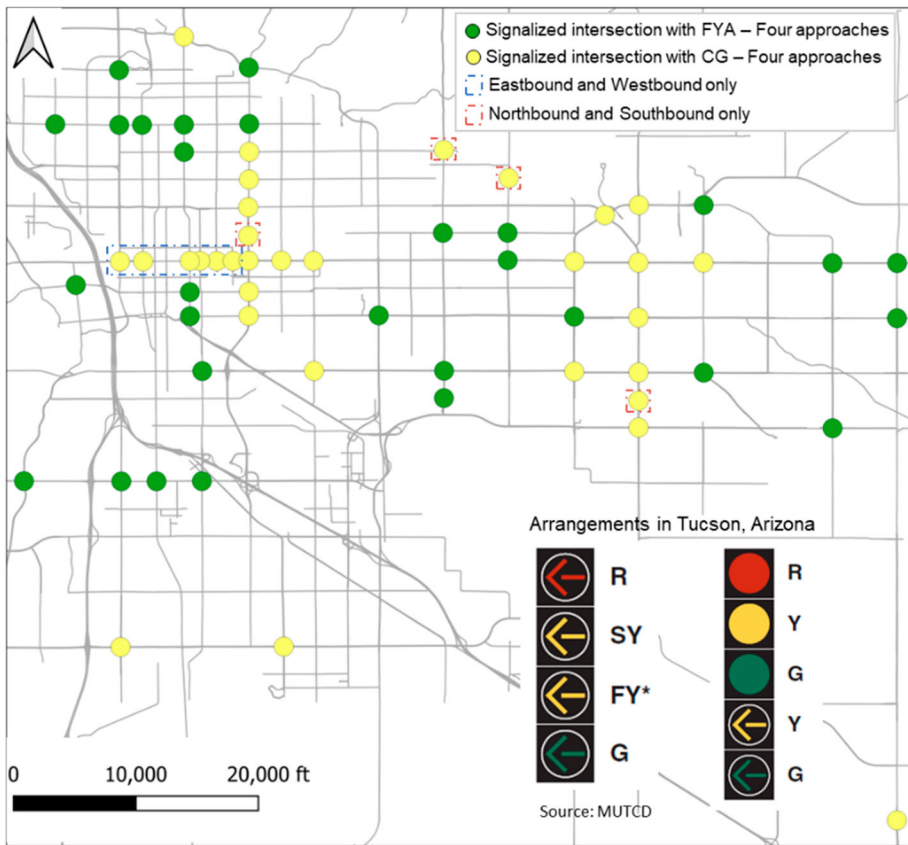


**Figure 1.** Study locations.

speeds of each vehicle (Islam and Abdel-Aty 2023). Vehicles equipped with inertial sensors that can report geolocations, speeds, accelerations, and others in near real-time to cloud infrastructure (Islam et al. 2023). Wejo processes real-time data from 11 million passenger vehicles from local streets to freeways (Kandiboina et al. 2024). The probe data is sampled at a rate of 3 s with a fidelity radius of 1.5 m (Islam and Abdel-Aty 2023; Saldivar-Carranza et al. 2021). A recent study confirmed the accuracy of Wejo data, showing that collected speeds were closely aligned with trends from traffic sensors (Kandiboina et al. 2024).

### 3.2.2. Traffic controller event-based data

The traffic controller event-based data was sourced from the Tucson Department of Traffic Mobility (TDTM). Most modern traffic signal controllers can collect and store high-resolution event logs (Liu et al. 2012) that record time-stamped phase changes and detector state transitions (Dobrota, Stevanovic, and Mitrovic 2024; Liu, Wang, and Jiang 2022). The event-based data is available for all intersections included in the study and contains timestamps of events, including 'Phase Begin Green,' 'Phase End Green,' and 'Phase Begin Red Clearance,' as logged by traffic controllers at signalised intersections. The permissive left-turn phase for approaches with CGs can be identified using the events 'Phase Begin Green' and 'Phase End Green.' Additionally, for approaches with FYAs, events such as 'FYA Begin Permissive'

TimeStamp	DeviceID	EventID	Parameter	EventID Reference
2022-01-07 05:40:53.500	6	1	4	Phase Begin Green
2022-01-07 05:40:53.500	6	1	8	Phase Begin Green
2022-01-07 05:40:53.500	6	33	1	FYA – End Permissive
2022-01-07 05:41:04.200	6	8	4	Phase Begin Yellow Clearance
2022-01-07 05:41:04.200	6	8	8	Phase Begin Yellow Clearance
2022-01-07 05:41:07.700	6	10	4	Phase Begin Red Clearance
2022-01-07 05:41:07.700	6	10	8	Phase Begin Red Clearance
2022-01-07 05:41:10.700	6	1	2	Phase Begin Green
2022-01-07 05:41:10.700	6	1	6	Phase Begin Green
2022-01-07 05:41:14.600	6	32	1	FYA – Begin Permissive

**Figure 2.** Sample event-based data.

and ‘FYA End Permissive’ have been logged and can be used to identify phases with FYA activated. Figure 2 shows sample events that have been logged by the controllers.

### 3.2.3. Traffic and geometric characteristics data

The speed data was obtained from INRIX through the Arizona Department of Transportation (ADOT). INRIX speed data compiles information from millions of GPS-enabled vehicles, mobile devices, conventional road sensors, historical traffic flow data from transportation agencies, and various other sources (INRIX 2023). These varied data sources are fused to provide real-time speed estimations (Kondyli, St. George, and Elefteriadou 2016). The speed data from INRIX is collected per minute per INRIX segment within Arizona. This study used INRIX speed data to represent the traffic state of the opposing traffic for each left-turn trajectory to high-level traffic conditions for road segments, consistent with other research approaches (He et al. 2023; Zhu et al. 2024). Additionally, the geometric characteristics, including speed limits, diagonal lengths of each intersection, the number of left-turn lanes, and the number of opposing through lanes, were manually collected from Google Maps.

### 3.3. Data processing

This study aimed to analyse the attributes of left-turning vehicles, including average speeds, maximum accelerations, and maximum decelerations. The typical left-turn maneuvers during permissive signal phases involve yielding to oncoming traffic when approaching the stop bar and proceeding through the intersection when drivers feel safe to complete the movement. Therefore, in this study, the impact of FYAs and CGs on left-turn behaviour was evaluated for the entering and leaving processes, as shown in Figure 3. The entering process involves driver actions in a zone that is 16 ft before and after the stop bar, as most hard accelerations have been observed within this zone (Saldivar-Carranza et al. 2021). Additionally, most vehicles slow down or stop in this area when yielding to oncoming traffic. Conversely, the leaving process involves driver actions in a zone extending from 16 ft after the stop bar to the first GPS point after turning into the target direction.



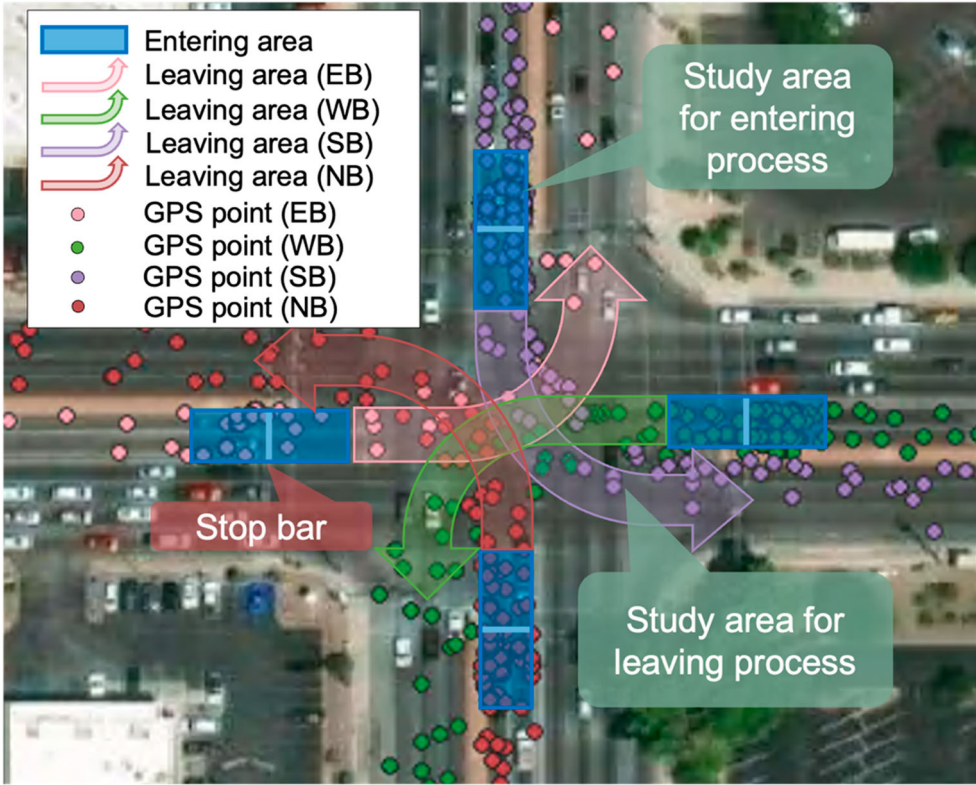


**Figure 3.** Sample trajectories from probe data and study area.

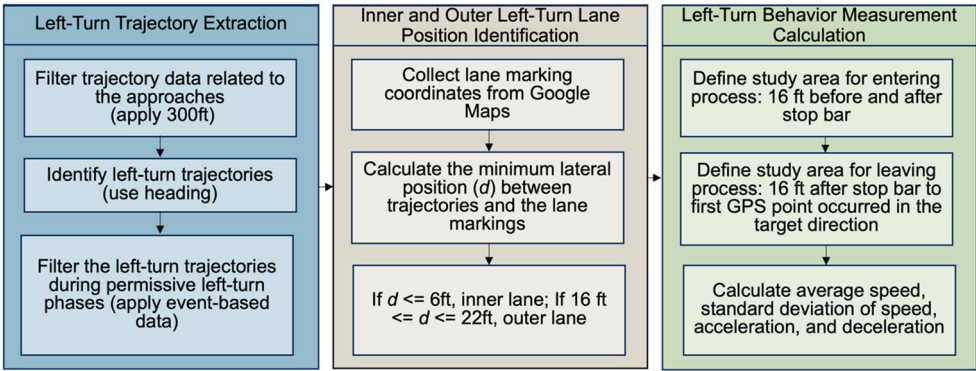


**Figure 4.** Steps for processing probe data.

Figure 4 illustrates the steps for calculating average speeds, maximum accelerations, and maximum decelerations from the trajectories. The process began with identifying left-turning vehicles during permissive left-turn phases. Once identified, the trajectories were labelled according to their positions in the inner or outer left-turn lanes. Finally, left-turn behaviour measures were calculated for each trajectory.



### **3.3.1. Left-turn trajectory extraction**

A total of 72,290 left-turn trajectories during permissive phases were analysed. Initially, a 300-foot buffer was applied to filter all GPS points in the probe data associated with the study intersections (Ryan et al. 2022; Zhang, Ryan, and Wu 2024). Vehicle headings were utilised to identify the left-turn trajectories for each intersection approach. Controller event-based data was then employed to filter the left-turn trajectories occurring during permissive left-turn phases. For each vehicle, if the timestamp of GPS points 32 ft before the stop bar fell within a permissive phase, and the timestamp of the first GPS point after turning into the target direction also fell within the same permissive phase, then this trajectory was considered to have completed the left-turn trajectory, i.e. had both entering and leaving processes, during the permissive phase and was used for subsequent analysis.

### **3.3.2. Inner and outer left-turn lane position identification**

To determine whether a vehicle was travelling in the inner or outer left-turn lane at an approach with dual left-turn lanes, the lateral distance between the lane markings of the solid yellow lane or median in the travel direction and the GPS points was calculated for each trajectory. This study found that lateral distances were less than 9 ft from the probe dataset for 49,047 left-turn trajectories occurring at 185 approaches with a single left-turn lane. Assuming a lane width of 12 ft (FHWA 2014) and accommodating GPS data errors, trajectories with a minimum lateral distance of less than 6 ft were labelled as being in the inner left-turn lane. Trajectories with a minimum lateral distance between 16 and 22 ft were labelled as being in the outer lane. Trajectories not meeting these criteria were excluded due to unclear lane information.

### **3.3.3. Left-turn behaviour measurement calculation**

The average speeds, maximum accelerations, and maximum decelerations were calculated for each left-turn trajectory for both the entering and leaving processes. For example, one trajectory included multiple GPS data points recorded during the entering process. The average speed of the trajectory was obtained by averaging the speeds associated with all GPS points. Accelerations and decelerations were derived from these speeds, and the maximum accelerations and decelerations for each trajectory were used in this study.

## **4. Methodology**

Tobit regression models with random effects and linear mixed-effects models were used to identify the impact of permissive left-turn indications (FYAs and CGs) and other factors on changes in driver behaviour. Subsequent sections provide details on the Tobit regression and linear mixed-effects models, model performance metrics, and the variables considered in the models.

### **4.1. Tobit regression model**

Tobit models were used to analyse factors affecting left-turn behaviour during the entering process. The Tobit regression model has been utilised in previous studies to handle the censoring problem (Anastasopoulos 2016; Anastasopoulos, Tarko, and Mannering 2008; Chen, Ma, and Chen 2014; Guo et al. 2019; Guo, Sayed, and Essa 2020; Hou, Huo, and Leng 2020;

Tobin 1958; Zeng et al. 2018, 2019). The Tobit model was selected because the left-turn behaviour measures (average speeds, maximum accelerations, and maximum decelerations) were continuous variables with many zeros during the entering process and were treated as left-censored (censored at zero) in this study. This observed pattern (many zero values) could be because left-turning vehicles tended to adhere to traffic rules by slowing down and stopping to yield to oncoming traffic when approaching intersections during permissive phases. Considering the possibility of unobserved heterogeneity across different approaches (Chen, Ma, and Chen 2014; Zhang, Ryan, and Wu 2024), Tobit regression models with random effects were employed in this study.

A baseline structure for a left-censored Tobit regression model was described as follows (Chen, Ma, and Chen 2014):

$$y_{it}^* = \beta x_{it} + \varepsilon_{it}, \quad i = 1, \dots, N; \quad t = 1, \dots, T_i \quad (1)$$

$$y_{it} = \begin{cases} 0 & \text{if } y_{it}^* \leq 0 \\ y_{it}^* & \text{if } y_{it}^* > 0 \end{cases} \quad (2)$$

where  $N$  is the total number of approaches,  $T_i$  is the total number of left-turn trajectories for each approach  $i$ ,  $y_{it}$  is the response variable (average speeds, maximum accelerations, and maximum decelerations),  $y_{it}^*$  is the latent variable that is observed only when it is positive,  $x_{it}$  is a vector of predictors (permissive left-turn indications, opposing through speeds, geometric characteristics, and temporal effects),  $\beta$  is a vector of estimable coefficients, and  $\varepsilon_{it}$  is the error term.

The Tobit regression model considering random effects was formed as:

$$\varepsilon_{it} = \mu_i + v_{it} \quad (3)$$

where  $\mu_i$  is the random effects term, which follows  $N(0, \sigma_\mu^2)$ ,  $v_{it}$  is the remaining disturbance term, which follows  $N(0, \sigma_v^2)$ , and  $\mu$  and  $v$  are independent.

The corresponding log-likelihood function for the Tobit regression model, considering random effects, was derived by obtaining the unconditional density through the integration of  $\mu_i$  out of the conditional density function (Greene 2012), as described below:

$$L_i = \int \prod_{y_{it}>0} \frac{1}{\sigma_v} \varphi\left(\frac{y_{it} - x'_{it}\beta - \mu_i}{\sigma_v}\right) \prod_{y_{it}=0} \Phi\left(\frac{-x'_{it}\beta - \mu_i}{\sigma_v}\right) \left(\frac{1}{\sigma_\mu}\right) \phi\left(\frac{1}{\sigma_\mu}\right) d\mu_i \quad (4)$$

$$\log L = \sum_{i=1}^N \log L_i \quad (5)$$

where  $x'_{it}$  is the vector of predictors in the Tobit regression model considering random effects,  $\varphi(*)$  is the standard normal density function, and  $\Phi(*)$  is the standard normal distribution function.

Additionally, Gauss-Hermite quadrature maximum likelihood estimation was adopted to obtain the maximum of the log-likelihood function of the Tobit regression model considering random effects (Greene 2012). Since the estimated parameters from the Tobit regression model cannot directly reflect the change in the response variable when the predictor increases by one unit (Anastasopoulos, Tarko, and Mannering 2008; Calzolari, Magazzini, and Meall 2001; Chen, Ma, and Chen 2014), the coefficients can be interpreted

in terms of their effect on the variable  $y^*$ . The latent variable marginal effects were given by:

$$\frac{\partial E[y_{it}^*]}{\partial x_{it}} = \beta \quad (6)$$

The marginal effects of a predictor on the expected value of the response variable were described as:

$$\frac{\partial E[y_{it}]}{\partial x_{it}} = \beta_i \Phi \left( \frac{x'_{it} \beta}{\sqrt{\sigma_\mu^2 + \sigma_v^2}} \right) \quad (7)$$

#### 4.2. Linear mixed-effects model

This study used a linear mixed-effects model with Lognormal distribution to account for unobserved heterogeneity across different approaches and to analyse the factors affecting left-turn behaviour during the leaving process. The left-turn behaviour measures were positive values during the leaving process and followed a slightly right-skewed normal distribution. The linear relationship among the log-transformed response variable and the fixed effects ( $\omega$ ) and random effects ( $\vartheta$ ) was defined as Equation (8) (Pinheiro and Bates 2000):

$$\ln(y_{it}) = \beta_0 + \beta x_{it} + \omega_i + \vartheta_{it} \quad (8)$$

where  $\omega_i$  is the random effect for the  $i$ th group;  $\vartheta_{it}$  is the residual error term. Both  $\omega_i$  and  $\vartheta_{it}$  are assumed to be normally distributed with a mean of 0, i.e.  $\omega_i \sim N(0, \sigma_\omega^2)$  and  $\vartheta_{it} \sim N(0, \sigma_\vartheta^2)$ . Marginal effects were estimated to interpret how average speeds, maximum accelerations, and maximum decelerations changed with a one-unit increase in the predictors.

#### 4.3. Model goodness-of-fit

The likelihood ratio test (LRT) was used to compare the performance of fixed-effects models against mixed-effects models. The LRT statistic was described as:

$$\chi^2 = -2[\log L(\beta_{m1}) - \log L(\beta_{m2})] \quad (9)$$

where  $\log L(\beta_{m1})$  is the log-likelihood at convergence for a fixed effects model one model, and  $\log L(\beta_{m2})$  is the log-likelihood at convergence for the mixed effects model. The test is chi-squared distributed, with degrees of freedom equal to the difference in the number of parameters between the two competing models. The test gives the level of confidence that one of the competing models is statistically superior to the other.

Moreover, Akaike Information Criterion (AIC) and Bayesian Information Criterion (BIC) were used to compare the goodness-of-fit of models:

$$AIC = 2k - 2 \log L \quad (10)$$

$$BIC = \log(n)k - 2 \log L \quad (11)$$

where  $n$  is the total number of left-turn trajectories, and  $k$  is the number of parameters in the model.

#### 4.4. Model variables

Regression models were developed for three response variables: average speeds, maximum accelerations, and maximum decelerations, separately. The explanatory variables included in these models were permissive left-turn indications (FYAs and CGs), opposing through speeds, number of left-turn lanes, number of opposing through lanes, speed limits, intersection size, time of day, and day of the week. Multicollinearity among explanatory variables was assessed using the Variance Inflation Factor (VIF). All VIF values for these predictors were found to be less than four, which is acceptable in previous transportation-related studies (Almasi and Behnood 2022; Zhang, Haule, and Wu 2025). Table 1 shows the summary statistics of the responses and explanatory variables.

### 5. Results and discussion

#### 5.1. Descriptive analysis

The study approaches had speed limits ranging from 30 to 45 mph, with the number of opposing through lanes ranging from one to three. To better understand the impact of permissive indications on left-turn behaviour at approaches with specific geometry, the study approaches were categorised into five groups based on their speed limits and the number of opposing through lanes, as described below:

- SL30-35&OT1 (Group1): Speed limits of 30–35 mph with one opposing through lane.
- SL30-35&OT2 (Group2): Speed limits of 30–35 mph with two opposing through lanes.
- SL30-35&OT3 (Group3): Speed limits of 30–35 mph with three opposing through lanes.
- SL40-45&OT2 (Group4): Speed limits of 40–45 mph with two opposing through lanes.
- SL40-45&OT3 (Group5): Speed limits of 40–45 mph with three opposing through lanes.

All categories except SL30-35&OT1 include both single left-turn approaches and dual left-turn approaches. SL30-35&OT1 includes approaches with a single left-turn lane. Results for SL30-35&OT2 and SL30-35&OT3 with dual left-turn lanes were excluded due to the limited number of left-turn trajectories. The top rows of Figures 5–10 are boxplots of the average speeds, maximum accelerations, and maximum decelerations of trajectories collected from approaches with FYAs and CGs. The descriptive analysis focused on data collected from weekdays, as weekdays typically have more fatalities than weekends (NHTSA 2024). The bottom rows show the results for inner and outer left-turn lanes of dual left-turn approaches. Additionally,  $p$ -values from Welch  $t$ -tests for comparison groups were included in the boxplots with deceleration values converted to positive for visualisation purposes.

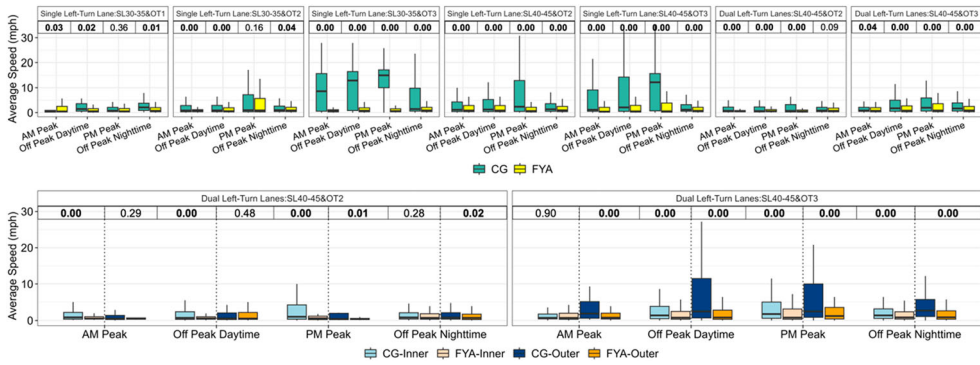
##### 5.1.1. Average speeds

Figure 5 depicts the average speeds during the entering process. Left-turning vehicles at approaches with a single left-turn lane and FYAs exhibited lower average speeds than those with CGs, particularly in SL30-35&OT3, SL40-45&OT2, and SL40-45&OT3. The differences in 85th percentile average speeds ranged from 3 to 16 mph. This suggests that, when approaching FYAs, drivers tended to reduce their speeds to yield more to oncoming traffic than when approaching CGs. Approaches with CGs showed greater variations in driver behaviour, with some maintaining higher speeds while others drove more slowly. This is

**Table 1.** Summary statistics of the analysis variables.

Variable		Description	Mean	Std	Min	Max	Count (Prop)
Entering process	Average speed	Average speed per trajectory (mph)	3.4	5.5	0.0	45.1	–
	Maximum acceleration	Maximum acceleration per trajectory ( $\text{m/s}^2$ )	0.2	0.3	0.0	2.9	–
	Maximum deceleration	Maximum deceleration per trajectory ( $\text{m/s}^2$ )	−0.3	0.4	−5.2	0.0	–
Leaving process	Average speed	Average speed per trajectory (mph)	14.8	4.9	5.0	36.5	–
	Maximum acceleration	Maximum acceleration per trajectory ( $\text{m/s}^2$ )	1.4	0.5	0.1	5.6	–
	Maximum deceleration	Maximum deceleration per trajectory ( $\text{m/s}^2$ )	−0.4	0.3	−5.2	−0.1	–
Opposing through speed		Opposing through speed during the left-turn process (mph)	29.2	6.7	7.0	54.0	–
Intersection size		Maximum diagonal of intersection (ft)	167.9	39.1	78.7	310.0	–
Permissive left-turn signal indication		CG	–	–	–	–	47,721 (66.0%)
	FYA	–	–	–	–	24,612 (34.0%)	
Number of left-turn lanes per approach		1	–	–	–	–	53,258 (73.6%)
	2	–	–	–	–	19,075 (26.4%)	
Number of opposing through lanes per approach		1	–	–	–	–	3868 (5.3%)
	2	–	–	–	–	43,311 (59.9%)	
	3	–	–	–	–	25,154 (34.8%)	
Speed limit		30 mph	–	–	–	–	3955 (5.5%)
	35 mph	–	–	–	–	18,230 (26.2%)	
	40 mph	–	–	–	–	40,739 (56.3%)	
	45 mph	–	–	–	–	9409 (13.0%)	
Time of day		AM peak (7–9 am)	–	–	–	–	7198 (10.0%)
	PM peak (4–6 pm)					8732 (12.1%)	
	Off-peak daytime (10 am to 3 pm)					32,359 (44.7%)	
	Off-peak nighttime (7 pm to 6 am)					24,004 (33.2%)	
Day of the week		Weekends	–	–	–	–	20,498 (28.3%)
	Weekdays	–	–	–	–	51,835 (71.7%)	

Note: Std: standard deviation; Prop: proportion.



**Figure 5.** Average speeds during the left-turn entering process.

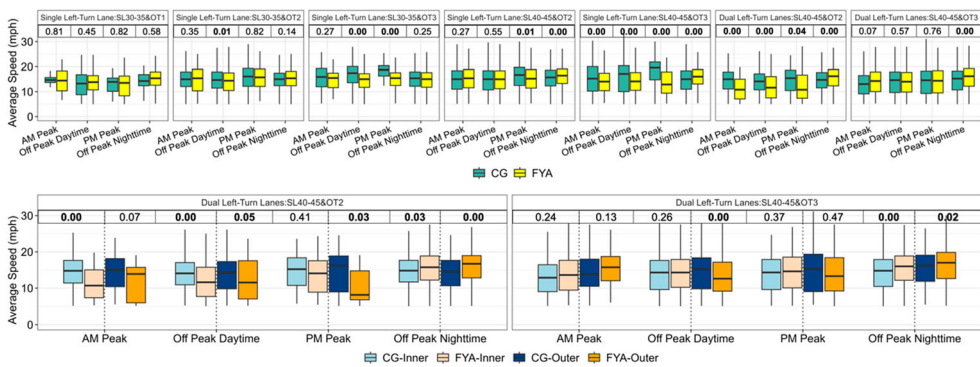


**Figure 6.** Average speeds during the left-turn leaving process.

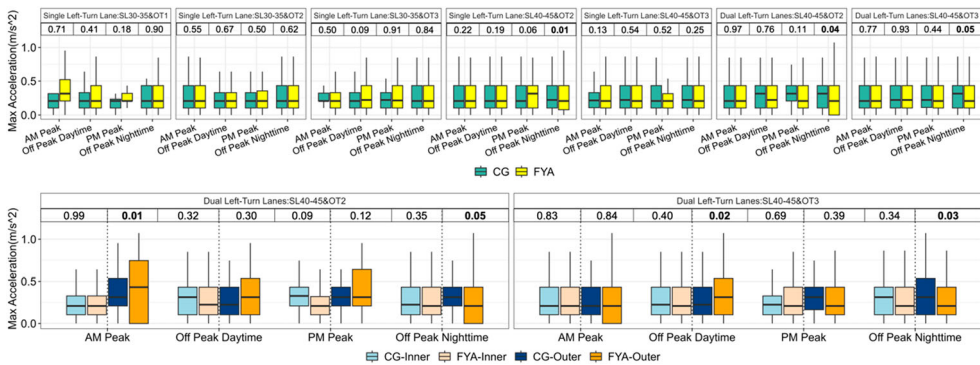


**Figure 7.** Maximum accelerations during the left-turn entering process.

potentially due to the confusion caused by CGs, consistent with findings from previous studies using driving simulators and surveys (Hurwitz et al. 2014; Knodler et al. 2005; Schattler et al. 2013). The inner and outer lanes with FYAs showed lower speeds than those with CGs.



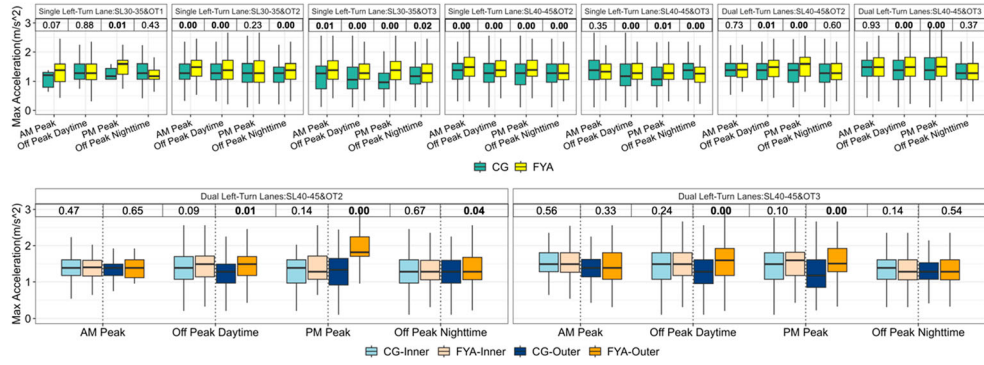


**Figure 8.** Maximum accelerations during the left-turn leaving process.

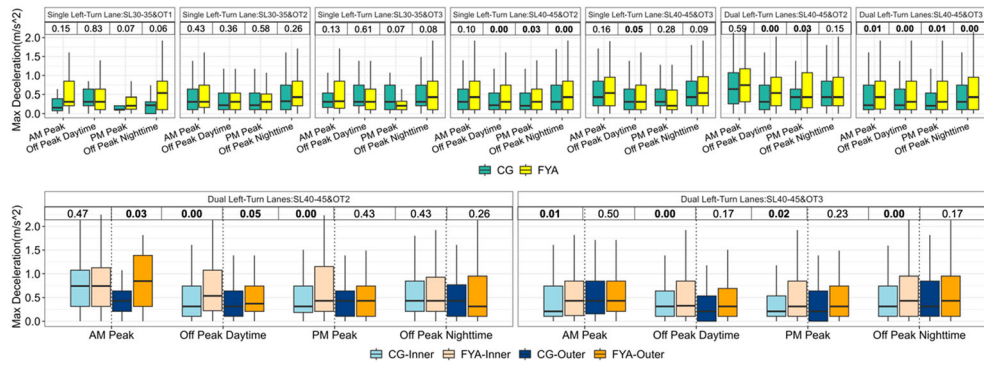


**Figure 9.** Maximum decelerations during the left-turn entering process.

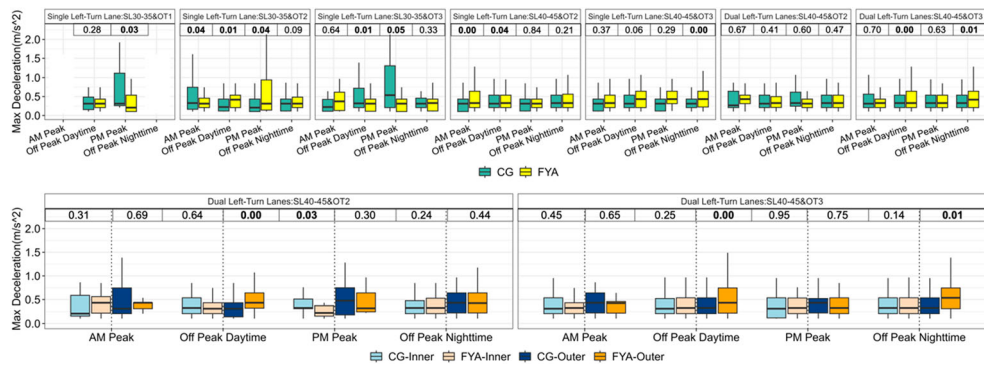


**Figure 10.** Maximum decelerations during the left-turn leaving process.

The average speeds during the entering process at dual left-turn lane approaches were lower than those at single left-turn approaches in SL40-45&OT2 and SL40-45&OT3. This could be attributed to drivers encroaching the intersection at slower speeds to gain a clearer view, which might have been limited by vehicles in the opposing left-turn lanes. Yan and Radwan (2007) showed that inadequate sight distance may cause cautious drivers

to reject physically adequate gaps because they need more time to ensure the opposing through lanes are clear (Yan and Radwan 2007). Similarly, Hutton et al. (2015) identified restricted sightlines caused by other left-turning vehicles as a significant issue (Hutton et al. 2015). Lower speeds in dual left-turn lanes may also result from the influence of adjacent vehicles. Drivers can be influenced by vehicles in the adjacent left-turn lane (Haglund and Åberg 2000; Lindorfer, Mecklenbraeuer, and Ostermayer 2017; Mohammadi et al. 2021). Dual left-turn lanes handle higher traffic volumes (X. Li et al. 2019), increasing the likelihood of drivers in both lanes turning simultaneously. These factors could cause drivers to approach dual left-turn intersections more cautiously, resulting in lower speeds than at single left-turn intersections.

Figure 6 shows that, during the leaving process, approaches with CGs had slightly higher speeds than those with FYAs, especially in inner lanes during AM peaks and daytime off-peaks (SL40-45&OT2) and in outer lanes during daytime off-peaks (SL40-45&OT2 and SL40-45&OT3) and PM peaks (SL40-45&OT2). This may be because about 50% of vehicles at CGs had higher entering speeds, while most vehicles at FYAs had speeds near 0 mph, as shown in Figure 5. This may lead drivers to maintain slightly higher speeds during the exiting process with CGs.

### 5.1.2. Maximum accelerations

Figure 7 shows lower accelerations for vehicles with FYAs than CGs on dual left-turn approaches in SL40-45&OT2 and SL40-45&OT3 during the nighttime off-peak periods. Vehicles in outer lanes with FYAs had higher accelerations than those with CGs during AM peaks and daytime off-peak periods, but lower accelerations during nighttime off-peak periods. All differences in accelerations ranged from 0.1–0.2 m/s<sup>2</sup>. An *F*-test revealed that outer lanes with FYAs showed higher fluctuations in accelerations compared to those with CGs. Local drivers were more accustomed to FYAs and likely adjusted their accelerations accordingly based on the gaps during the day, while commuters from surrounding jurisdictions that lack FYAs might be slower to react. Studies suggest that familiarity is often reflected in changes in driving behaviour, attention to the external environment, and perception of the driving conditions (Intini, Colonna, and Ryeng 2019; Young et al. 2018).

Figure 8 shows that left-turning vehicles with FYAs generally had higher accelerations than those with CGs during the leaving process. Accelerations of outer lanes with FYAs during PM peaks in SL40-45&OT2 exceeded the 2.6 m/s<sup>2</sup>, a threshold used in previous studies to denote hard accelerations (Hunter et al. 2021; Saldivar-Carranza et al. 2021). This may be attributed to driver behaviour impacted by traffic flow states (G. Li et al. 2020) and local drivers' familiarity (Intini, Colonna, and Ryeng 2019; Young et al. 2018) with the driving environment and signal indications. Moreover, as observed in this study, the speeds of most drivers entering approaches with FYAs were lower than those with CGs, which may lead to higher accelerations as they resumed travel.

### 5.1.3. Maximum decelerations

Figure 9 shows that during the entering process, left-turning vehicles on approaches with FYAs exhibited higher decelerations compared to those on approaches with CGs, especially in SL40-45&OT2 (single left-turn lane) and SL40-45&OT3 (dual left-turn lanes). The differences in decelerations ranged from 0.1–1.0 m/s<sup>2</sup>. Left-turning vehicles in both inner and outer lanes with FYAs exhibited slightly higher decelerations compared to those on

**Table 2.** Model goodness-of-fit measures.

Model comparisons	Tobit regression model (entering process)						Linear mixed-effects model (leaving process)					
	Avg. speed		Max. accel- eration		Max. decel- eration		Avg. speed		Max. accel- eration		Max. decel- eration	
	F.E.	R.E.	F.E.	R.E.	F.E.	R.E.	F.E.	R.E.	F.E.	R.E.	F.E.	R.E.
AIC	3055	3015	1296	1284	1616	1601	387	378	503	490	204	203
BIC	3057	3017	1297	1285	1618	1603	388	380	504	491	205	205

Note: F.E.: fixed effects; R.E.: fixed effects incorporating random effects; AIC: Akaike Information Criterion; BIC: Bayesian Information Criterion.

approaches with CGs. Similarly, Figure 10 shows that, during the leaving process, left-turning vehicles on single left-turn approaches with FYAs had slightly higher decelerations than those with CGs, especially in SL30-35&OT2 during daytime off-peak periods and PM peaks, in SL40-45&OT2 during AM peaks, and in SL40-45&OT3 during nighttime off-peak periods. Conversely, during the leaving process, left-turning vehicles on single left-turn approaches with FYAs had slightly lower decelerations than those with CGs in SL30-35&OT1 during the PM peaks, in SL30-35&OT2 during AM peaks, and in SL30-35&OT3 during daytime off-peak periods and PM peaks.

**5.2. Model results**

Regression models were used to evaluate the impact of FYAs and CGs on left-turning vehicles’ speeds, accelerations, and decelerations when entering and leaving the intersections. These models accounted for the influence of various factors, including opposing traffic attributes, approach geometries, time of day, and day of the week. The AIC, BIC, and LRT statistics were used to assess the models’ goodness-of-fit. The LRT results, with all *p*-values below 0.05, demonstrated that models incorporating random effects offered a better fit to the data than models with fixed effects. Table 2 shows that models with random effects had better model fits over their fixed-effects counterparts based on the AIC and BIC results. Therefore, the next subsections present and discuss the impact of several factors on left-turn behaviour based on the mixed-effects models shown in Table 3. Results in Table 3 are displayed in terms of the marginal effects for the response variables, as derived from these mixed-effects models. The random effects parameters were significant in all models, indicating the significance of unobserved heterogeneity in the findings.

**5.2.1. Permissive left-turn indications**

Compared to CGs, FYAs tended to reduce the average speeds and accelerations of left-turning vehicles during the entering process by 2.564 mph and 0.012 m/s<sup>2</sup>, respectively. Earlier studies suggested this difference stemmed from drivers’ interpretation of FYAs as a yield condition versus CGs as a directive to proceed (Brehmer 2003; Knodler et al. 2006). This study’s findings demonstrated drivers’ continued heightened awareness of the need to yield, even as these signals have become more familiar to the driving public, consistent with a recent study in Minnesota (Koch 2024). Despite documented increases in aggressive driving behaviour following the COVID-19 pandemic (FHWA 2024), FYAs remain effective at promoting a more cautious behaviour compared to CGs. While Schattler et al. (2013) found

**Table 3.** Summary of model results.

Model results		Entering process (marginal effects)			Leaving process (marginal effects)		
	Avg. speed	Max. acceleration	Max. deceleration	Avg. speed	Max. acceleration	Max. deceleration	
Constant		1.997**	0.291**	0.117**	2.578**	0.198**	−1.824**
Permissive left-turn signal indications	CG <sup>a</sup>						
	FYA	−2.564**	−0.012*	0.047**	−0.023	0.059*	0.071
Opposing through speed (mph)		−0.069**	0.000	0.001**	−0.0001	0.001**	0.003*
Number of left-turn lanes	1 <sup>a</sup>						
	2	−1.058**	0.006	−0.023**	−0.035**	0.016*	−0.061**
Number of opposing through lanes	1 <sup>a</sup>						
	2	1.395**	−0.041**	0.056**	−0.014	0.026**	0.068*
	3	1.754**	−0.041**	0.106**	−0.002	0.027**	0.101**
Speed limit (mph)	30 <sup>a</sup>						
	35	−1.390**	−0.013	0.064**	0.028**	−0.052**	0.104
	40	−1.216**	−0.014	0.054	0.037**	−0.088**	0.048
	45	−1.937**	−0.026	0.085**	0.076**	−0.009	0.051
Intersection size (ft)		0.024**	0.000	0.001**	0.0001	0.000	0.002**
Time of day	AM peak <sup>a</sup>						
	PM peak	1.463**	0.005	−0.099**	0.021**	−0.043**	−0.019
	Daytime Off-peak	0.512**	0.003	−0.094**	−0.034**	−0.015**	0.018
	Nighttime Off-peak	−0.356**	0.008	−0.002	0.033**	−0.043**	0.045
Day of the week	Weekends <sup>a</sup>						
	Weekdays	0.623**	−0.003	−0.011**	0.008**	−0.006	0.005
$\sigma_{\mu}$		1.774**	0.022**	0.776**	0.068**	0.106**	0.124**
$\sigma_{\nu}$		5.203**	0.292**	5.199**	0.365**	0.413**	0.732**

Note: \* $p < 0.1$ ; \*\* $p < 0.05$ ; a: the reference group in the regression models.

no significant differences in traffic operations between FYAs and CGs in terms of gap acceptance, red-light running, and yellow-light running (Schattler et al. 2013), this study observed significant variations in vehicle speeds across left-turning vehicles with CGs compared to FYAs. This finding has important safety implications, as crash severity is closely related to vehicle speeds at the time of collision (Tefft 2011). By encouraging lower left-turn speeds, FYAs might lower the severity of crashes at intersections than CGs. A detailed comparison of crash severity at intersections with FYAs versus CGs could further confirm the impact of these signals on safety.

Understanding how FYAs and CGs influence left-turning vehicles when leaving the intersection is crucial for enhancing the safety of downstream road users, especially pedestrians. Previous research often neglected to assess left-turn driver behaviour during this departure phase. This study found that FYAs increased vehicle accelerations by  $0.59 \text{ m/s}^2$  compared to CGs during departure, consistent with the results shown in Figure 8. This may be due to lower entry speeds at approaches with FYAs, requiring greater acceleration to complete left turns. Additionally, this effect could be influenced by traffic flow conditions (G. Li et al. 2020) and drivers' familiarity with the driving environment and signal indications (Intini, Colonna, and Ryeng 2019; Young et al. 2018).

### 5.2.2. Geometric attributes

Compared to single left-turn approaches, dual left-turn approaches tended to lower vehicles' average speeds by 1.058 and 0.035 mph during the entering and leaving process, respectively. This suggests drivers may traverse dual left-turn lanes at lower speeds, possibly due to reduced visibility, driver interactions with one another (Mohammadi et al. 2021), and potentially more queued vehicles at dual left-turn lanes (X. Li et al. 2019). A unit increase in opposing through speeds was correlated with a 0.069 mph decrease in the left-turning vehicles' entering speeds.

Approaches with two or three opposing through lanes had higher average speeds during the entering process compared to those with one opposing lane. While more opposing through lanes typically accommodate more traffic, drivers entering these approaches could maintain higher speeds because larger intersections with more lanes often have higher posted speed limits. If they enter the approach with a sufficient gap, they can make their turns without significantly slowing down. A study revealed that as speed limits increase, critical gaps also increase (Claros et al. 2021).

During the leaving process, dual left-turn approaches tended to exhibit higher accelerations than single left-turn lanes by  $0.016 \text{ m/s}^2$ . This increase in acceleration may be attributed to the necessity for vehicles to compensate for lower speeds at dual left-turn approaches. Approaches with speed limits of 35 and 40 mph were associated with lower accelerations than those with a 30-mph speed limit. A study revealed that posted speed limits significantly affected gap acceptance parameters. As speed limits decrease, critical gaps also decrease, potentially indicating drivers to accelerate more quickly at intersections with lower speed limits (Claros et al. 2021). Moreover, Hutton et al. (2015) estimated opposing vehicle speeds using the posted speed limit when analysing left-turn lane offset (Hutton et al. 2015). Higher speed limits, on the other hand, may result in faster entry and departure speeds for left-turning vehicles.

Dual left-turn approaches exhibited lower decelerations than single left-turn approaches during both entering and leaving. Left-turning vehicles at approaches with dual left-turn

lanes tended to have lower speeds and, hence, did not require higher decelerations when observing potential conflicts. Larger intersections were associated with higher decelerations for left-turning vehicles. Compared to one opposing through lane, two and three opposing through lanes increased decelerations by 0.056 and 0.106 m/s<sup>2</sup>, respectively, during the entering process, and by 0.068 and 0.101 m/s<sup>2</sup> during leaving. Approaches with 35 and 45 mph speed limits increased decelerations by 0.064 and 0.085 m/s<sup>2</sup>, respectively, compared to those with a 30-mph speed limit. A unit increase in opposing through speeds resulted in a 0.001 m/s<sup>2</sup> increase in decelerations during entering and a 0.003 m/s<sup>2</sup> increase during leaving.

### 5.2.3. Temporal effects

PM peaks showed a 1.463 mph increase in entering speeds and 0.021 mph in leaving speeds compared to AM peaks. Daytime off-peak periods saw a 0.512 mph increase in entering speeds but a 0.034 mph decrease in leaving speeds. Nighttime off-peak periods decreased entering speeds by 0.356 mph and increased leaving speeds by 0.033 mph. Weekdays had higher entering speeds by 0.623 mph and leaving speeds by 0.008 mph compared to weekends. This might be because drivers value their time more during peak periods than on weekends (Dixit, Gayah, and Radwan 2012), which could lead them to drive slightly faster on weekdays for commuting.

AM peaks typically exhibited higher accelerations and decelerations. Compared to AM peaks, non-AM peak periods tended to decrease leaving accelerations by 0.015–0.043 m/s<sup>2</sup> and entering decelerations by 0.002–0.094 m/s<sup>2</sup>. These observations are consistent with prior research indicating more aggressive driver behaviour during morning peaks (Dixit, Gayah, and Radwan 2012). This may be due to the morning commute often being associated with increased negative emotions, such as anger, frustration, and depression (Kandiboina et al., 2024).

## 6. Conclusions

Left-turn movements at signalised intersections, especially during permissive left-turn phases, have presented significant safety concerns due to potential conflicts with oncoming traffic and pedestrians. Adopting the flashing yellow arrow (FYA) as a permissive left-turn indication has improved intersection safety by lowering crash frequency compared to a circular green signal (CG). However, further understanding of the influence of FYAs on left-turn driver behaviour, including average speeds, accelerations, and decelerations, is needed. This study leveraged probe data and employed descriptive and regression analyses to comprehensively assess the influence of FYAs on left-turn behaviour. Left-turning drivers' speeds, accelerations, and decelerations when entering and leaving intersections with FYAs and CGs were evaluated. Regression models incorporated various attributes, including the number of left-turn lanes, the number of opposing through lanes, approach speed limits, opposing through speeds, intersection sizes, time of day, and day of the week.

The findings from the descriptive and regression analyses indicated that left-turning vehicles at approaches with FYAs exhibited lower average speeds during entering and leaving processes than those with CGs. This trend was also observed for both single left-turn and dual left-turn approaches, and the inner and outer lanes of dual left-turn approaches. Compared to CGs, left-turning vehicles on approaches with FYAs exhibited slightly lower



accelerations during the entering process and slightly higher accelerations during the leaving process. Vehicles on dual left-turn lanes with FYAs had marginally lower accelerations than those with CGs during the entering process. However, the vehicles in the outer lanes of dual left-turn approaches demonstrated significant fluctuations in accelerations compared to those with CGs. This variability may be attributed to drivers in outer lanes, with FYAs being influenced by varying sight visibility and behaviour while creeping forward. During the leaving process, accelerations in outer lanes with FYAs, particularly at approaches with 40–45 mph speed limits and two opposing through lanes during PM peaks, tended to be classified as hard accelerations. Moreover, vehicles on approaches with FYAs had slightly higher decelerations during both entering and leaving processes than those on approaches with CGs. During entry, vehicles in the inner and outer lanes of dual left-turn lanes had higher decelerations with FYAs compared to CGs.

Findings showed that vehicles on dual left-turn lanes had lower average speeds during entry, particularly with FYAs, compared to single left-turn approaches. This suggests drivers tended to navigate dual left-turn approaches at significantly reduced speeds. The dual left-turn approaches also showed lower decelerations during the entering and leaving processes. Therefore, deploying FYAs at approaches with dual left-turn lanes may not necessarily compromise intersection safety, especially during entry. Instead, it could achieve a balance between safety and mobility at intersections. However, during the leaving process, compared to single left-turn approaches, vehicles on dual left-turn lanes exhibited higher accelerations.

Trends observed in this study suggest that FYAs had varying influences on left-turn behaviour at approaches with different geometries. This study acknowledges limitations, including the lack of consideration for spatial relationships between approaches and the resolution of the probe data. While a previous study also estimated accelerations using Wejo data (Joshi et al. 2025), the 3s resolution makes it challenging to accurately capture hard decelerations and accelerations. However, this limitation does not affect the comparison between the impact of FYAs and CGs, as the measures from these two groups followed the same calculation methods. Future studies exploring vehicle movements can take into account the number of queued vehicles. The results provide detailed insights into the effects of FYAs at the driver's level, considering geometric configurations, opposing traffic conditions, time of day, and day of the week. Transportation agencies may use the study findings when deciding FYA deployments to improve intersection safety.

## Acknowledgments

The authors would like to gratefully thank the City of Tucson for providing event-based data and technical assistance. Special thanks to PAG and ADOT for their support with probe data and INRIX speed data.

## Disclosure statement

No potential conflict of interest was reported by the author(s).

## References

Abou-Senna, H., J. Hibbert, E. Radwan, H. Eldeeb, and A. Hashim. 2023. "Evaluation of Dynamic Flashing Yellow Arrow Decision Support System in the Field Using Before and After Real-Time

- Data." *Transportation Research Record* 2677 (8): 676–690. <https://doi.org/10.1177/03611981231157724>.
- Abou-Senna, H., E. Radwan, and H. Eldeeb. 2021. "A Peer-to-Peer Logic Environment to Validate Flashing Yellow Arrow Decision Support System." *Journal of Traffic and Transportation Engineering (English Edition)* 8 (5): 735–750. <https://doi.org/10.1016/j.jtte.2020.06.001>.
- Abou-Senna, H., E. Radwan, R. C. Harb, A. Navarro, and S. Chalise. 2014. "Interactive Decision Support System for Predicting Flashing Yellow Arrow Left-Turn Mode by Time of Day." *Transportation Research Record* 2463 (1): 16–25. <https://doi.org/10.3141/2463-03>.
- Alhajyaseen, W. K., M. Asano, and H. Nakamura. 2013. "Left-Turn Gap Acceptance Models considering Pedestrian Movement Characteristics." *Accident Analysis & Prevention* 50:175–185. <https://doi.org/10.1016/j.aap.2012.04.006>.
- Almasi, S. A., and H. R. Behnood. 2022. "Exposure-Based Geographic Analysis Mode for Estimating the Expected Pedestrian Crash Frequency in Urban Traffic Zones: Case Study of Tehran." *Accident Analysis & Prevention* 168: 106576. <https://doi.org/10.1016/j.aap.2022.106576>.
- Anastasopoulos, P. C. 2016. "Random Parameters Multivariate Tobit and Zero-Inflated Count Data Models: Addressing Unobserved and Zero-State Heterogeneity in Accident Injury-Severity Rate and Frequency Analysis." *Analytic Methods in Accident Research* 11:17–32. <https://doi.org/10.1016/j.amar.2016.06.001>.
- Anastasopoulos, P. C., A. P. Tarko, and F. L. Mannering. 2008. "Tobit Analysis of Vehicle Accident Rates on Interstate Highways." *Accident Analysis & Prevention* 40 (2): 768–775. <https://doi.org/10.1016/j.aap.2007.09.006>.
- Appiah, J., F. A. King, M. D. Fontaine, and B. H. Cottrell. 2018. "Safety Effects of Flashing Yellow Arrows Used in Protected Permitted Phasing: Comparison of Full Bayes and Empirical Bayes Results." *Transportation Research Record* 2672 (21): 20–29.
- Appiah, J., F. A. King, M. D. Fontaine, and B. H. Cottrell. 2020. "Left Turn Crash Risk Analysis: Development of a Microsimulation Modeling Approach." *Accident Analysis and Prevention* 144:105591. <https://doi.org/10.1016/j.aap.2020.105591>.
- Brehmer, C. L. 2003. *Evaluation of Traffic Signal Displays for Protected/Permissive Left-Turn Control*. Vol. 493. Transportation Research Board.
- Calzolari, G., L. Magazzini, and F. Meall. 2001. "Simulation-Based Estimation of Tobit Model with Random Effects." *Econometric Studies: A Festschrift in Honour of Joachim Frohn* 8:349.
- Chan, C. Y. 2006. "Characterization of Driving Behaviors Based on Field Observation of Intersection Left-Turn Across-Path Scenarios." *IEEE Transactions on Intelligent Transportation Systems* 7 (3): 322–331. <https://doi.org/10.1109/tits.2006.880638>.
- Chen, F., X. Ma, and S. Chen. 2014. "Refined-scale Panel Data Crash Rate Analysis Using Random-Effects Tobit Model." *Accident Analysis & Prevention* 73:323–332. <https://doi.org/10.1016/j.aap.2014.09.025>.
- Claros, B., M. Chitturi, A. Bill, and D. A. Noyce. 2021. "Impact of Geometry and Operations on Left-Turn Gap Acceptance at Signalized Intersections with Permissive Indication." *Transportation Research Record* 2675 (10): 367–380. <https://doi.org/10.1177/03611981211011476>.
- Dixit, V. V., V. V. Gayah, and E. Radwan. 2012. "Comparison of Driver Behavior by Time of Day and Wet Pavement Conditions." *Journal of Transportation Engineering* 138 (8): 1023–1029. [https://doi.org/10.1061/\(asce\)jte.1943-5436.0000400](https://doi.org/10.1061/(asce)jte.1943-5436.0000400).
- Dobrota, N., A. Stevanovic, and N. Mitrovic. 2024. "A Novel Model to Jointly Estimate Delay and Arrival Patterns by Using High-Resolution Signal and Detection Data." *Transportmetrica A: Transport Science* 20 (1): 2047126. <https://doi.org/10.1080/23249935.2022.2047126>.
- FHWA. 2014. *Lane Width*. [https://safety.fhwa.dot.gov/geometric/pubs/mitigationstrategies/chapter3/3\\_lanewidth.cfm](https://safety.fhwa.dot.gov/geometric/pubs/mitigationstrategies/chapter3/3_lanewidth.cfm)
- FHWA. 2024. *About Intersection Safety*. <https://highways.dot.gov/safety/intersection-safety/about>.
- Greene, W. 2012. *Limdep, Version 10.0*. Plainview, NY: Econometric Software, Inc.
- Guo, Y., Z. Li, P. Liu, and Y. Wu. 2019. "Modeling Correlation and Heterogeneity in Crash Rates by Collision Types Using Full Bayesian Random Parameters Multivariate Tobit Model." *Accident Analysis & Prevention* 128:164–174. <https://doi.org/10.1016/j.aap.2019.04.013>.

- Guo, Y., T. Sayed, and M. Essa. 2020. "Real-Time Conflict-Based Bayesian Tobit Models for Safety Evaluation of Signalized Intersections." *Accident Analysis & Prevention* 144:105660. <https://doi.org/10.1016/j.aap.2020.105660>.
- Haglund, M., and L. Åberg. 2000. "Speed Choice in Relation to Speed Limit and Influences from Other Drivers." *Transportation Research Part F: Traffic Psychology and Behaviour* 3 (1): 39–51. [https://doi.org/10.1016/S1369-8478\(00\)00014-0](https://doi.org/10.1016/S1369-8478(00)00014-0).
- He, C., D. Wang, M. Chen, G. Qian, and Z. Cai. 2023. "Link Dynamic Vehicle Count Estimation Based on Travel Time Distribution Using License Plate Recognition Data." *Transportmetrica A: Transport Science* 19 (2): 2012299. <https://doi.org/10.1080/23249935.2021.2012299>.
- Hou, Q., X. Huo, and J. Leng. 2020. "A Correlated Random Parameters Tobit Model to Analyze the Safety Effects and Temporal Instability of Factors Affecting Crash Rates." *Accident Analysis & Prevention* 134:105326. <https://doi.org/10.1016/j.aap.2019.105326>.
- Hunter, M., E. Saldivar-Carranza, J. Desai, J. K. Mathew, H. Li, and D. M. Bullock. 2021. "A Proactive Approach to Evaluating Intersection Safety Using Hard-Braking Data." *Journal of Big Data Analytics in Transportation* 3 (2): 81–94. <https://doi.org/10.1007/s42421-021-00039-y>.
- Hunter, M. P., S. K. Wu, H. K. Kim, and W. Suh. 2012. "A Probe-Vehicle-Based Evaluation of Adaptive Traffic Signal Control." *IEEE Transactions on Intelligent Transportation Systems* 13 (2): 704–713. <https://doi.org/10.1109/tits.2011.2178404>.
- Hurwitz, D. S., C. M. Monsere, P. Marnell, and K. Paulsen. 2014. "Three-or Four-Section Displays for Permissive Left Turns?" *Transportation Research Record: Journal of the Transportation Research Board* 2463 (1): 1–9. <https://doi.org/10.3141/2463-01>.
- Hutton, J. M., K. M. Bauer, C. A. Fees, and A. Smiley. 2015. "Evaluation of Left-Turn Lane Offset Using the Naturalistic Driving Study Data." *Journal of Safety Research* 54:5–e1. <https://doi.org/10.1016/j.jsr.2015.06.016>.
- INRIX. 2023. *INRIX Analytics: Speed*. <https://inrix.com/products/speed/>.
- Intini, P., P. Colonna, and E. O. Ryeng. 2019. "Route Familiarity in Road Safety: A Literature Review and an Identification Proposal." *Transportation Research Part F: Traffic Psychology and Behaviour* 62:651–671. <https://doi.org/10.1016/j.trf.2018.12.020>.
- Islam, Z., and M. Abdel-Aty. 2023. "Traffic Conflict Prediction Using Connected Vehicle Data." *Analytic Methods in Accident Research* 39:100275. <https://doi.org/10.1016/j.amar.2023.100275>.
- Islam, Z., M. Abdel-Aty, N. Anwari, and M. R. Islam. 2023. "Understanding the Impact of Vehicle Dynamics, Geometric and Non-Geometric Roadway Attributes on Surrogate Safety Measure Using Connected Vehicle Data." *Accident Analysis & Prevention* 189:107125. <https://doi.org/10.1016/j.aap.2023.107125>.
- Joshi, M., A. Bamney, K. Wang, S. Zhao, J. Ivan, and E. Jackson. 2025. "Analyzing the Suitability of Vehicle Telematics Data as a Surrogate Safety Measure for Short-Term Crashes." *Transportation Research Record* 2679 (2): 489–504.
- Kandiboina, R., S. Knickerbocker, S. Bhagat, N. Hawkins, and A. Sharma. 2024. "Exploring the Efficacy of Large-Scale Connected Vehicle Data in Real-Time Traffic Applications." *Transportation Research Record* 2678 (5): 651–665. <https://doi.org/10.1177/03611981231191512>.
- Knodler Jr, M. A., D. A. Noyce, K. C. Kacir, and C. L. Brehmer. 2005. "Evaluation of Flashing Yellow Arrow in Traffic Signal Displays with Simultaneous Permissive Indications." *Transportation Research Record* 1918 (1): 46–55.
- Knodler Jr, M. A., D. A. Noyce, K. C. Kacir, and C. L. Brehmer. 2006. "Analysis of Driver and Pedestrian Comprehension of Requirements for Permissive Left-Turn Applications." *Transportation Research Record* 1982 (1): 65–75.
- Koch, S. 2024. *Do Drivers Understand Flashing Yellow Arrows? U Research Offers Guidance for Local Agencies*. Accessed June. <https://www.cts.umn.edu/news-pubs/news/2024/May/arrows>
- Kondyli, A., B. St. George, and L. Eleftheriadou. 2016. "Comparison of Travel Time Measurement Methods Along Freeway and Arterial Facilities." *Transportation Letters* 10 (4): 215–228. <https://doi.org/10.1080/19427867.2016.1245259>.
- Li, P., M. Abdel-Aty, Q. Cai, and C. Yuan. 2020. "The Application of Novel Connected Vehicles Emulated Data on Real-Time Crash Potential Prediction for Arterials." *Accident Analysis & Prevention* 144:105658. <https://doi.org/10.1016/j.aap.2020.105658>.

- Li, G., W. Lai, X. Sui, X. Li, X. Qu, T. Zhang, and Y. Li. 2020. "Influence of Traffic Congestion on Driver Behavior in Post-Congestion Driving." *Accident Analysis & Prevention* 141:105508. <https://doi.org/10.1016/j.aap.2020.105508>.
- Li, H., J. Mathew, W. Kim, and D. Bullock. 2020. "Using Crowdsourced Vehicle Braking Data to Identify Roadway Hazards."
- Li, X., A. Weber, A. Cottam, and Y.-J. Wu. 2019. "Impacts of Changing from Permissive/Protected Left-Turn to Protected-Only Phasing: Case Study in the City of Tucson, Arizona." *Transportation Research Record: Journal of the Transportation Research Board* 2673 (4): 616–626. <https://doi.org/10.1177/0361198119842108>.
- Li, X., S. Yu, Y. Lei, N. Li, and B. Yang. 2024. "Dynamic Vision-Based Machinery Fault Diagnosis with Cross-Modality Feature Alignment." *IEEE/CAA Journal of Automatica Sinica* 11 (10): 2068–2081. <https://doi.org/10.1109/JAS.2024.124470>.
- Li, X., W. Zhang, X. Li, and H. Hao. 2023. "Partial Domain Adaptation in Remaining Useful Life Prediction with Incomplete Target Data." *IEEE/ASME Transactions on Mechatronics* 29 (3): 1903–1913.
- Lindorfer, M., C. F. Mecklenbraeuer, and G. Ostermayer. 2017. "Modeling the Imperfect Driver: Incorporating Human Factors in a Microscopic Traffic Model." *IEEE Transactions on Intelligent Transportation Systems* 19 (9): 2856–2870. <https://doi.org/10.1109/TITS.2017.2765694>.
- Liu, H. X., W. Ma, X. Wu, and H. Hu. 2012. "Real-Time Estimation of Arterial Travel Time under Congested Conditions." *Transportmetrica* 8 (2): 87–104. <https://doi.org/10.1080/18128600903502298>.
- Liu, S., Z. Wang, and H. Jiang. 2022. "Signal Timing Optimisation with the Contraflow Left-Turn Lane Design Using the Cell Transmission Model." *Transportmetrica A: Transport Science* 18 (3): 1254–1277. <https://doi.org/10.1080/23249935.2021.1936280>.
- Ma, Y., and J. Zhu. 2021. "Left-turn Conflict Identification at Signal Intersections Based on Vehicle Trajectory Reconstruction under Real-Time Communication Conditions." *Accident Analysis & Prevention* 150:105933. <https://doi.org/10.1016/j.aap.2020.105933>.
- Mathew, J. K., H. Li, H. Landvater, and D. M. Bullock. 2022. "Using Connected Vehicle Trajectory Data to Evaluate the Impact of Automated Work Zone Speed Enforcement." *Sensors (Basel)* 22 (8): 2885. <https://doi.org/10.3390/s22082885>.
- Mohammadi, S., R. Arvin, A. J. Khattak, and S. Chakraborty. 2021. "The Role of Drivers' Social Interactions in Their Driving Behavior: Empirical Evidence and Implications for Car-Following and Traffic Flow." *Transportation Research Part F: Traffic Psychology and Behaviour* 80:203–217. <https://doi.org/10.1016/j.trf.2021.04.002>.
- NHTSA. 2024. *Early Estimate of Motor Vehicle Traffic Fatalities in 2023*. National Highway Traffic Safety Administration.
- Pinheiro, J. C., and D. M. Bates. 2000. "Linear Mixed-Effects Models: Basic Concepts and Examples." In *Mixed-Effects Models in S and S-Plus*. Statistics and Computing, 3–56. New York, NY: Springer. [https://doi.org/10.1007/978-1-4419-0318-1\\_1](https://doi.org/10.1007/978-1-4419-0318-1_1).
- Rescot, R., S. Qu, R. Noteboom, and A. Nafakh. 2015. *Evaluation of Flashing Yellow Arrow Traffic Signals in Indiana*. FHWA/IN/JTRP-2015/08.
- Rietgraf, A., and K. L. Schattler. 2013. "Behavior of Left-Turning Drivers during Permissive Interval of Protected–Permissive Operation." *Transportation Research Record: Journal of the Transportation Research Board* 2384 (1): 35–44. <https://doi.org/10.3141/2384-05>.
- Rodegerdts, L. A., B. Nevers, B. Robinson, J. Ringert, P. Koonce, J. Bansen, ... K. G. Courage. 2004. *Signalized Intersections: Informational Guide*. No. FHWA-HRT-04-091. United States. Department of Transportation. Federal Highway Administration, Turner-Fairbank Highway Research Center.
- Ryan, A., C. Ai, C. Fitzpatrick, and M. Knodler. 2022. "Crash Proximity and Equivalent Property Damage Calculation Techniques: An Investigation Using a Novel Horizontal Curve Dataset." *Accident Analysis & Prevention* 166:106550. <https://doi.org/10.1016/j.aap.2021.106550>.
- Saldivar-Carranza, E. D., J. K. Mathew, H. Li, M. Hunter, T. Platte, and D. M. Bullock. 2021. "Using Connected Vehicle Data to Evaluate Traffic Signal Performance and Driver Behavior after Changing Left-Turns Phasing." In *2021 IEEE International Intelligent Transportation Systems Conference (ITSC)*. Indianapolis, IN, USA: IEEE.

- Schattler, K. L., C. J. Gulla, T. J. Wallenfang, B. A. Burdett, and J. A. Lund. 2015. "Safety Effects of Traffic Signing for Left Turn Flashing Yellow Arrow Signals." *Accident Analysis and Prevention* 75:252–263. <https://doi.org/10.1016/j.aap.2014.11.010>.
- Schattler, K. L., A. Rietgraf, B. Burdett, and W. Lorton. 2013. *Driver Comprehension and Operations Evaluation of Flashing Yellow Arrows*. ICT-13-021 UILU-ENG-2013-2018.
- Srinivasan, R., B. Lan, D. Carter, S. Smith, and K. Signor. 2018. "Crash Modification Factors for the Flashing Yellow Arrow Treatment at Signalized Intersections." *Transportation Research Record* 2672 (30): 142–152.
- Tefft, B. C. 2011. *Impact Speed and a Pedestrian's Risk of Severe Injury or Death*. Technical Report. Washington, DC: AAA Foundation for Traffic Safety.
- Tobin, J. 1958. "Estimation of Relationships for Limited Dependent Variables." *Econometrica: Journal of the Econometric Society* 26 (1): 24–36. <https://doi.org/10.2307/1907382>.
- Wang, B., Y. Liu, G. Liang, and Y. Men. 2023. "Behavior-Based Safety Evaluation Model of Vehicles Turning Left at Intersections with a Permitted Left-Turn Phase." *Journal of Transportation Engineering, Part A: Systems* 149 (9): 04023091. <https://doi.org/10.1061/jtepbs.Teeng-7753>.
- Yan, X., and E. Radwan. 2007. "Effect of Restricted Sight Distances on Driver Behaviors during Unprotected Left-Turn Phase at Signalized Intersections." *Transportation Research Part F: Traffic Psychology and Behaviour* 10 (4): 330–344. <https://doi.org/10.1016/j.trf.2007.01.001>.
- Young, A. H., A. K. Mackenzie, R. L. Davies, and D. Crundall. 2018. "Familiarity Breeds Contempt for the Road Ahead: The Real-World Effects of Route Repetition on Visual Attention in an Expert Driver." *Transportation Research Part F: Traffic Psychology and Behaviour* 57:4–9. <https://doi.org/10.1016/j.trf.2017.10.004>.
- Zeng, Q., Q. Guo, S. C. Wong, H. Wen, H. Huang, and X. Pei. 2019. "Jointly Modeling Area-Level Crash Rates by Severity: A Bayesian Multivariate Random-Parameters Spatio-Temporal Tobit Regression." *Transportmetrica A: Transport Science* 15 (2): 1867–1884. <https://doi.org/10.1080/23249935.2019.1652867>.
- Zeng, Q., H. Wen, H. Huang, X. Pei, and S. C. Wong. 2018. "Incorporating Temporal Correlation Into a Multivariate Random Parameters Tobit Model for Modeling Crash Rate by Injury Severity." *Transportmetrica A: Transport Science* 14 (3): 177–191. <https://doi.org/10.1080/23249935.2017.1353556>.
- Zhang, X., H. Haule, and Y. J. Wu. 2025. "Investigating the Impact of Pedestrian Hybrid Beacons on the Effectiveness of Adaptive Traffic Control Systems." *Journal of Transportation Engineering, Part A: Systems* 151 (5): 04025025. <https://doi.org/10.1061/JTEPBS.TEENG-8661>.
- Zhang, X., X. Li, and Y.-J. Wu. 2023. "Safety Performance Evaluation of Flashing Yellow Arrow: Time-of-Day versus 24-Hour Operation." *Transportation Research Record: Journal of the Transportation Research Board* 2677 (7): 420–433. <https://doi.org/10.1177/03611981231152461>.
- Zhang, X., A. Ryan, and Y.-J. Wu. 2024. "Influential Factors of Pedestrian and Bicycle Crashes Near Pedestrian Hybrid Beacons: Observing Trends through an Applied Analysis." *Journal of Transportation Safety & Security* 16 (11): 1307–1330. <https://doi.org/10.1080/19439962.2024.2325399>.
- Zhao, J., V. L. Knoop, J. Sun, Z. Ma. 2023. "Unprotected Left-Turn Behavior Model Capturing Path Variations at Intersections." *IEEE Transactions on Intelligent Transportation Systems* 24 (9): 9016–9030.
- Zhu, Z., S. Zhu, L. Sun, and A. Mardan. 2024. "Modelling Changes in Travel Behaviour Mechanisms through a High-Order Hidden Markov Model." *Transportmetrica A: Transport Science* 20 (1): 2130731. <https://doi.org/10.1080/23249935.2022.2130731>.